THE APPROACH TO REMOTE SENSING OF WATER VAPOR BASED ON GPS AND LINEAR REGRESSION T_m IN EASTERN REGION OF CHINA

Li Jianguo (李建国) and *Mao Jietai* (毛节泰)

LSSR*, Department of Geophysics, Peking University, Beijing 100871

Received November 15, 1997; revised April 25, 1998

ABSTRACT

The approach to remote sensing of water vapor by using global positioning systems (GPS) is discussed. In order to retrieve the vertical integrated water vapor (IWV) or the precipitable water (PW), the weighted "mean temperature" of the atmosphere, T_m would be estimated to the specific area and season. T_m depends on surface temperature, tropospheric temperature profile, and the vertical distribution of water vapor. The surface temperature dependence is borne out by a comparison of T_m and the values of surface temperature T_s using radiosonde profiles of Beijing Station (No. 54511) throughout 1992. The analysis of radiosonde profiles spanning a one-year interval (1992) from sites in eastern region of China with a latitude range of 20 − 50°N and a longitude range of 100 − 130°E yields the coefficients a and b of a linear regression equation $T_m = a + bT_s$.

Key words: global positioning system (GPS), vertical integrated water vapor, weighted mean temperature

I. INTRODUCTION

Water vapor plays an essential role in many processes of atmospheric physics and atmospheric chemistry. It is the most important greenhouse gas, and is also the major factor which influences the accuracy in short-term forecasts of precipitation. In addition, water vapor affects the vertical stability of the atmosphere, the structure and evolution of atmospheric storm systems and the earth's meridian energy balance. Therefore meteorologists pay serious attention to the measurement of water vapor content and its distribution.

Water vapor is the most variable element of major constituents of the atmosphere. Because the temporal and spatial variabilities of water vapor are much finer than those of temperature and wind, the contemporary radiosonde measurement inadequately resolves such variability of water vapor. Water vapor can be measured using microwave radiometers. Ground-based microwave radiometers provide a good temporal but poor spatial coverage, whereas satellite-based units have the opposite characteristics. Satellite-based units tend to be more useful over oceans than over land. As a tool of remote sensing

* LSSR is acronym of Laboratory for Severe Storm Research.

of atmospheric water vapor. GPS does not have such serious disadvantages. Therefore it is the best device.

GPS was originally designed as a navigational and time transfer system, but it is now widely employed by geodesists, geophysicists, and surveyors. In order to be able to remove the atmospheric effects on microwave transfer as a "noise", geodesists and geophysicists have spent a great deal of effort. However, meteorologists just utilize such effects for exploiting GPS as a means of studying the atmospheric characteristics. Meteorologists and GPS specialists working together should be able to design procedures that can be used to characterize the troposphere in detail.

II. THE APPROACH TO THE REMOTE SENSING OF ATMOSPHERIC WATER VAPOR USING GPS

The approach of the remote sensing of atmospheric water vapor was advanced by Bevis et al. (1992). Mao (1993) also discussed this approach in detail. In this article we only present a brief description of the approach.

1. *Atmospheric Propagation Delay, Zenith Delay and Mapping Function*

The approach to the remote sensing of atmospheric water vapor using GPS is based on the physics of electric wave propagation in atmosphere. Due to the atmospheric effect, time-lagged radio signals that propagated from GPS satellites to the ground-based GPS receivers would bring about propagation delay that was caused either by that waves travel in a curved path instead of in a straight line, or by that waves travel slower than they would in vacuum. Propagation delay depends on the distribution of refractivity. Time delay is equivalent to the increase of propagation path. The excess path length is given by

$$\Delta L = c_0\int \frac{\mathrm{d}s}{c} - G, \tag{1}$$

where G is the geometrical distance between GPS satellites and GPS receivers. Introducing the atmospheric refractivity $N=10^6\times(n-1)$, here n is atmospheric index of refraction, and neglecting the difference between the curved path length and geometrical distance, Eq. (1) is replaced by

$$\Delta L = 10^{-6}\times\int N(s)\mathrm{d}s, \tag{2}$$

where the integral is made along the curved ray path.

The total atmospheric delay ΔL consists of both "hydrostatic delay" ΔL_h and "wet delay" ΔL_w. ΔL_h is a larger quantity which depends only on surface pressure. ΔL_w is a smaller quantity which is a function of water vapor distribution. In the zenith direction, the total delay is minimal. Let ΔL^0 represent the zenith total delay. Then

$$\Delta L^0 = 10^{-6}\times\int_0^\infty N(z)\mathrm{d}z. \tag{3}$$

The integral is made along the zenith path. Atmospheric total delay ΔL can be written as

$$\Delta L = m(\varepsilon)\Delta L^0, \tag{4}$$

where ε is the elevation angle of the GPS satellites. The $m(\varepsilon)$ is known as the "mapping function", depending on the elevation angle ε. Denoting the "zenith hydrostatic delay" and "zenith wet delay" as ΔL_h^0 and ΔL_w^0, respectively, we have

$$\Delta L = m_h(\varepsilon)\Delta L_h^0 + m_w(\varepsilon)\Delta L_w^0, \quad (5)$$

where $m_h(\varepsilon)$ and $m_w(\varepsilon)$ are the hydrostatic and wet mapping functions, respectively. Davis et al. (1985) showed the following form of mapping function

$$m_h(\varepsilon) = \frac{1}{\sin\varepsilon + \cfrac{a}{\tan\varepsilon + \cfrac{b}{\sin\varepsilon + c}}}, \quad (6)$$

$$\begin{aligned} a = {} & 0.001185[1 + 0.6071 \times 10^{-4}(P_0 - 1000) \\ & - 0.1471 \times 10^{-3}e_0 + 0.3072 \times 10^{-2}(T_0 - 20) \\ & + 0.1965 \times 10^{-1}(\beta + 6.5) - 0.5645 \times 10^{-2}(h_t - 11.231)], \\ b = {} & 0.001144[1 + 0.1164 \times 10^{-4}(P_0 - 1000) + 0.2795 \times 10^{-3}e_0 \\ & + 0.3109 \times 10^{-2}(T_0 - 20) + 0.3038 \times 10^{-1}(\beta + 6.5) \\ & - 0.1217 \times 10^{-1}(h_t - 11.231)], \\ c = {} & -0.0090, \end{aligned}$$

where P_0 is the total surface pressure in hPa, e_0 is the partial pressure of water vapor at the surface (in hPa), t_0 is the surface temperature in Centigrade, β is the tropospheric temperature lapse rate in K km^{-1}, and h_t is the height of the tropopause in km.

The mapping functions m_h and m_w are similar above the elevation angle of 10—15°.

2. *Atmospheric Refractivity, Zenith Hydrostatic Delay and Zenith Wet Delay*

In order to determine the zenith total delay ΔL_0, we must know the distribution of atmospheric refractivity. The three-term formula for the total refractivity of moist air, as given by Thayer (1974) can be written as

$$N = k_1 \frac{P_d}{T} Z_d^{-1} + k_2 \frac{P_w}{T} Z_w^{-1} + k_3 \frac{P_w}{T^2} Z_w^{-1}, \quad (7)$$

where T is temperature, P_d and P_w are the partial pressures of the dry constituents and the water vapor, respectively. Z_d and Z_w are the compressibilities, with the subscripts having the same meaning as for partial pressure. k_1, k_2 and k_3 can be expressed as

$$\begin{aligned} k_1 &= 77.604 \pm 0.014 \ (\mathrm{K\ hPa^{-1}}), \\ k_2 &= 64.79 \pm 0.08 \ (\mathrm{K\ hPa^{-1}}), \\ k_3 &= 377600 \pm 400 \ (\mathrm{K^2\ hPa^{-1}}). \end{aligned}$$

The values for k_2 and k_3, which have been obtained by measurements in the microwave region are different, e. g., Birnbaum and Chatterjee (1952) found $k_2 = (71.4 \pm 5.8)$ K hPa^{-1} and $k_3 = (3.747 \pm 0.029) \times 10^5$ K^2 hPa^{-1}, while Boudouris (1963) found $k_2 = (72 \pm 11)$ K hPa^{-1} and $k_3 = (3.75 \pm 0.03) \times 10^5$ K^2 hPa^{-1}. Owens (1967) proposed the expressions for the inverse compressibility Z_d^{-1} for dry air and Z_w^{-1} for water vapor by least squares fitting of thermodynamic data. These expressions are

$$Z_d^{-1} = 1 + P_d\left[57.97 \times 10^{-8}\left(1 + \frac{0.52}{T}\right) - 9.4611 \times 10^{-4} \frac{t}{T^2}\right], \quad (8)$$

$$Z_w^{-1} = 1 + 1650\left(\frac{e}{T^3}\right)[1 - 0.01317t + 1.75 \times 10^{-4}t^2 + 1.44 \times 10^{-6}t^3], \quad (9)$$

where t is the temperature in Centigrade. P_d and P_w are in hPa and T is in K.

Integration of the refractivity in (7) requires knowledge of the profiles of both the wet and dry constituents, and the mixing ratio. Davis et al. (1985) rewrote the first two terms in (7) by using the equation of state as

$$k_1 \frac{P_d}{T} Z_d^{-1} + k_2 \frac{P_w}{T} Z_w^{-1} = k_1 R_d \rho_d + k_2 R_w \rho_w = k_1 R_d \rho + k'_2 \frac{P_w}{T} Z_w^{-1}, \tag{10}$$

where $\rho = \rho_d + \rho_w$ is the total mass density, and the coefficient k'_2 is given by

$$k'_2 = k_2 - k_1 \frac{R_d}{R_w} = k_2 - k_1 \frac{M_w}{M_d}, \tag{11}$$

where R_d is the specific gas constant for dry air, and R_w is the specific gas constant for water vapor. M_d and M_w are the molecular weights of dry air and water vapor, respectively. Thus the total refractivity is given by

$$N = k_1 R_d \rho + k'_2 \frac{P_w}{T} Z_w^{-1} + k_3 \frac{P_w}{T^2} Z_w^{-1}. \tag{12}$$

The first term in (12) is dependent only on the total density, but not on the wet/dry mixing ratio. This term can be integrated by applying the condition of hydrostatic equilibrium. Davis et al. (1985) has given the zenith hydrostatic delay

$$\Delta L_h^0 = [(0.0022768 \pm 0.0000005)\text{m hPa}^{-1}] \frac{P_0}{f(\lambda, H)}, \tag{13}$$

where ΔL_h^0 is in m, and P_0 is the surface pressure in hPa, while $f(\lambda, H) = 0.0026\cos 2\lambda - 0.00028H$, with λ being the geodetic site latitude and H is the height in km of the station above the geoid.

The remaining two terms in (7) are wet terms

$$N_w = \left(k'_2 \frac{P_w}{T} + k_3 \frac{P_w}{T^2} \right) Z_w^{-1}. \tag{14}$$

And ΔL_w^0 is determined by numerical integration of the wet refractivity given in (14) using radiosonde profiles of P_w and T, thus

$$\Delta L_w^0 = 10^{-6} \int_0^\infty N_w \mathrm{d}z = 10^{-6} \int_0^\infty \left(k_2' \frac{P_w}{T} + k_3 \frac{P_w}{T^2} \right) Z_w^{-1} \mathrm{d}z = 10^{-6} Z_w^{-1} \left(k_2' + \frac{k_3}{T_m} \right) \int_0^\infty \frac{P_w}{T} \mathrm{d}z, \tag{15}$$

where T_m is

$$T_m = \frac{\int_0^\infty \frac{P_w}{T} \mathrm{d}z}{\int_0^\infty \frac{P_w}{T^2} \mathrm{d}z}, \tag{16}$$

and is called as "the weighted mean temperature" of the atmosphere. Let $k_3' = k_3/T_m + k_2'$. Because Z_w^{-1} is very close to 1, (15) can be rewritten as

$$\Delta L_w^0 = 10^{-6} k_3' \int_0^\infty \frac{P_w}{T} \mathrm{d}z. \tag{17}$$

3. *The Remote Sensing of Atmospheric Water Vapor*

In order to represent the water vapor content of atmosphere, Bevis et al. (1992) introduced the vertically integrated water vapor (IWV) which is the mass of vapor per unit area and the precipitable water (PW) which is the height of an equivalent column of water. Using the equation of state for water vapor, Bevis et al. (1992) obtained

$$\int_0^\infty \frac{P_w}{T}dz = R_w\int_0^\infty \rho_w dz = R_w \times IWV. \tag{18}$$

Substituting (18) into (17), we have

$$\Delta L_w^0 = 10^{-6}\left(\frac{k_3}{T_m} + k'_2\right)R_w \times IWV, \tag{19}$$

or

$$IWV = k\Delta L_w^0, \tag{20}$$

where $1/k = [10^{-6}(k_3/T_m + k'_2)]R_w$. Numerically, the IWV is just the product of ρ and PW, that is

$$PW = \frac{IWV}{\rho}, \tag{21}$$

where ρ is the density of water. Equations (20) and (21) are basic equations for the remote sensing of atmospheric water vapor using the ground-based GPS.

III. THE LINEAR REGRESSION OF T_m

If ΔL_w^0 is given by GPS observation and the constant k is determined by T_m, we can retrieve IWV from (20). Therefore "the weighted mean temperature" T_m is the crucial parameter to estimate the vertical integral water vapor IWV.

If we choose a single value of T_m for all areas and seasons, the accuracy in remote sensing of the atmospheric water vapor would be not only crucially decreased, but also it can not depict the temporal and spatial changes. Therefore there is no any practical worth for a single value of T_m.

Because water vapor mainly concentrates in the troposphere, especially in the lower troposphere, and a large fraction of wet delay is produced in the troposphere, specially in the lower troposphere, so it is possible to estimate the T_m from (16) using the radiosonde profiles of P_w and T. But there are only twice daily radiosonde data for an observatory,

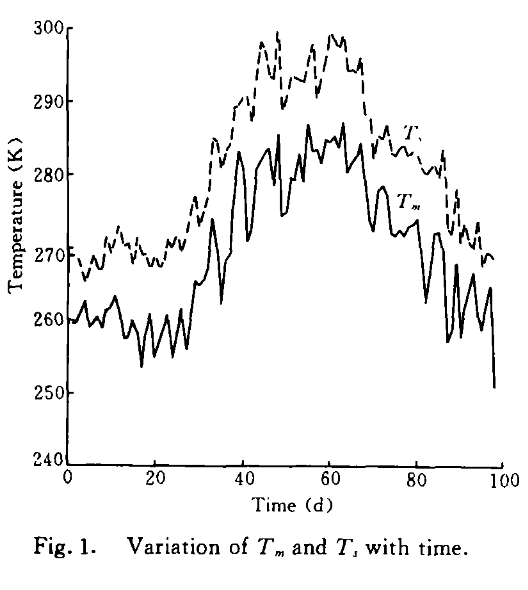

Fig. 1. Variation of T_m and T_s with time.

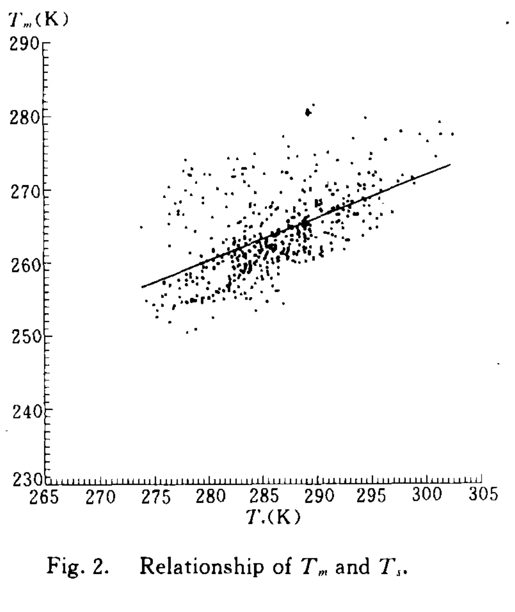

Fig. 2. Relationship of T_m and T_s.

and stations are sparse, therefore the temporal and spatial resolution of T_m is poorer.

Bevis et al. (1992) indicated that T_m depends on the surface temperature, tropospheric temperature profile, and vertical distribution of water vapor. Therefore an alternative approach would be used to estimate the T_m on basis of the surface temperature.

First, as a special example, we give the temporal variation of T_m and T_s in Fig. 1, where T_m was obtained from 98 available radiosonde profiles of P_w and T from Beijing Observatory in 1992. The value of surface temperature T_s was reported at the time of release. Figure 1 shows that change of T_m is in good agreement with the T_s. This result for the dependence of T_m on T_s yields the following linear equation

$$T_m = a + bT_s. \tag{22}$$

By the least square approach, the value of $\sum_i^n [T_{m,i} - (a + bT_{s,i})]^2$ must be minimal for the values of coefficients a and b, so we have

$$b = \frac{T_{sm}}{T_{ss}}, \tag{23a}$$

$$a = \langle T_m \rangle - b\langle T_s \rangle, \tag{23b}$$

where

$$\langle T_s \rangle = \frac{1}{n}\sum_{i=1}^{n} T_{s,i}, \qquad \langle T_m \rangle = \frac{1}{n}\sum_{i=1}^{n} T_{m,i},$$

$$T_{ss} = \sum_{i=1}^{n} (T_{s,i} - \langle T_s \rangle)^2, \qquad T_{sm} = \sum_{i=1}^{n} (T_{s,i} - \langle T_s \rangle)^2 (T_{m,i} - \langle T_m \rangle).$$

Based on these equations and using the radiosonde data from observatories in eastern China, we can obtain the coefficients a and b by month in this area. The values of a and b are presented in Table 1. In this table we also give the standard deviation and the number of samples. Making use of this table, we can easily obtain the regression equation between T_m and T_s. For example, $T_m = 96.56 + 0.58T_s$ for September. Figure 2 represents the linear fitting between T_m and T_s. Slope of the fitting straight line is 0.58. The points in Fig. 2 were evaluated using radiosonde profiles from every observatory in this region.

This approach has serious defects. Because the most water vapor is located in the first 2—3 km of the lower atmosphere, the large vertical intervals of radiosonde data exist and the distribution of observatory is sparse, it is not favorate to accurately estimate the effect of water vapor.

The temporal and spatial resolution of the data available from observational network is lower. We use a mesoscale meteorological model MM4 to generate fields of meteorological variables with a 100 km resolution encompassing the eastern part of China. A high resolution planetary boundary layer (PBL) is utilized. The model has 15 vertical layers between the ground and the 100 hPa pressure surface. A terrain-following coordinate system is used in which the vertical coordinate, σ, is equal to $(P - P_{top})/(P_{surf} - P_{top})$, where P_{surf} and P_{top} are the surface pressure and 100 hPa pressure, respectively. P is the pressure at the surface where σ is evaluated. The vertical resolution of the model is variable. The resolution near the surface is higher than that at upper levels. It is more reasonable to estimate the distribution of water vapor. In this study, the center of grid domain is at 35°N and 115°E. Maximum of grid point is 31×31, the interval of grids is 100

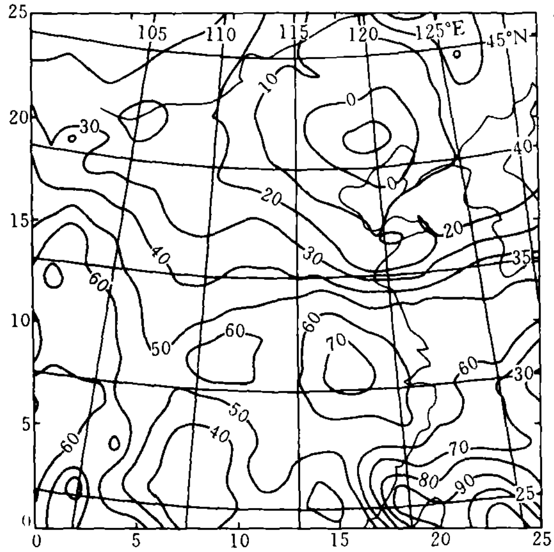

Fig. 3. Year-averaged domain distribution of coefficient a.

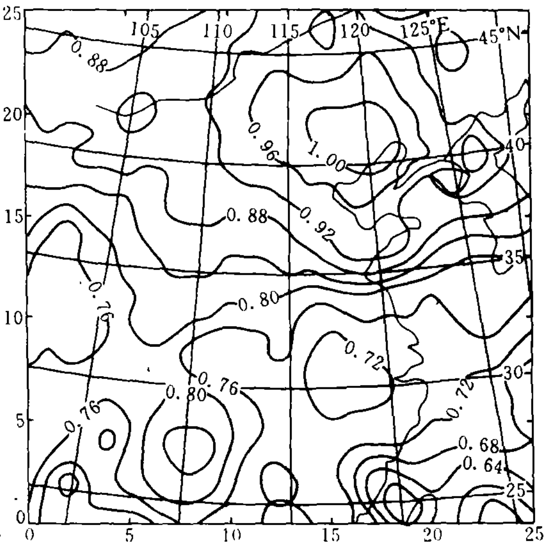

Fig. 4. Year-averaged domain distribution of coefficient b.

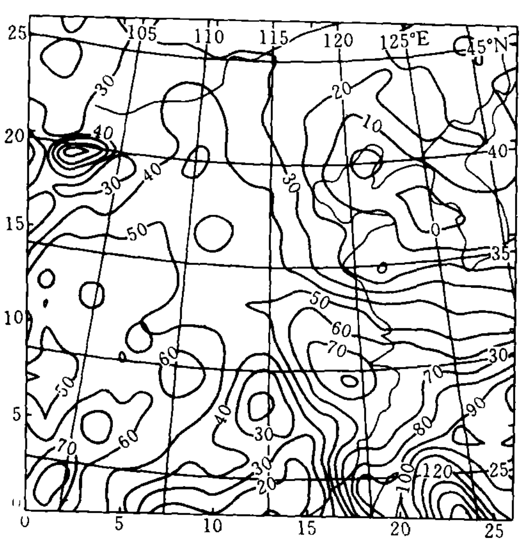

Fig. 5. The domain distribution of coefficient a (September).

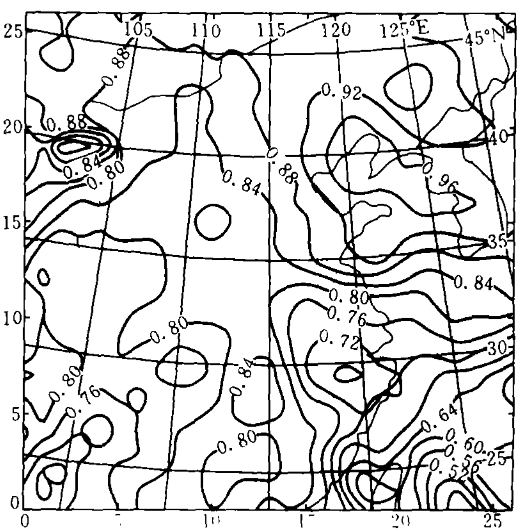

Fig. 6. The domain distribution of coefficient b (September).

km. Meteorological inputs for the model are the radiosonde and surface observational data in 1992 and in the region over which the model is being applied. The T_m is estimated by (16) using the temperature and humidity data that were output by MM4. We ultimately obtain year-averaged values of a and b over each subgrid area and the entire grid domain.

The domain distribution of year-averaged values of a and b is represented in Figs. 3 and 4. respectively. The month-averaged and year-averaged values of a and b over the entire model domain are represented in Table 2. In addition, we also give the standard deviation, residual standard deviation, and the correlation coefficients in this table. From

Table 2 we can easily obtain. for example. the regression equation for total year- and domain-averaged values of T_m and T_s. It is given

$$T_m = 44.05 + 0.81T_s. \tag{24}$$

Equation (24) applies to all year and entire grid domain. We can obtain coefficients a and b that applies to all the year and every subgrid region from Fig. 3 and Fig. 4. Thereby regression equation that applies to all the year and every subgrid region is obtained. We also estimate monthly domain distribution of coefficients a and b. For example, Fig. 5 and Fig. 6 show domain distribution of a and b for September, respectively. Thus we can get regression equation that applies to every subgrid region and every month. It improves the temporal and spatial resolution of T_m.

Table 1. Coefficients a and b from Radiosonde Data

	Jan.	Feb.	Mar.	Apr.	May	Jun.	Jul.	Aug.	Sep.	Oct.	Nov.	Dec.
a	202.81	188.81	98.65	163.51	233.19	196.80	163.10	193.02	96.56	166.12	117.97	139.11
b	0.20	0.24	0.56	0.34	0.11	0.24	0.37	0.26	0.58	0.34	0.50	0.42
SD	1.65	1.92	3.60	1.89	0.97	1.24	1.46	0.86	3.12	1.96	4.32	3.69
NS	1816	1188	644	729	682	714	477	571	520	913	670	794

Note: SD is standard deviation in K. and NS is number of sample.

Table 2. Coefficients a and b from Meteorological Model

	Jan.	Feb.	Mar.	Apr.	May	Jun.	Jul.	Aug.	Sep.	Oct.	Nov.	Dec.	year
a	64.38	49.92	47.47	43.10	41.97	40.77	40.12	40.33	40.50	39.93	39.80	40.31	44.05
b	0.73	0.9	0.80	0.81	0.82	0.82	0.82	0.82	0.82	0.82	0.82	0.82	0.81
SD	2.80	4.01	3.41	3.43	3.08	2.56	2.27	1.92	2.61	2.94	3.62	2.92	2.96
RSD	1.19	1.29	1.09	1.06	0.86	0.79	0.75	0.63	0.74	1.31	1.52	1.54	1.06
R	0.91	0.95	0.95		0.95	0.95	0.94	0.91	0.96	0.91	0.92	0.87	0.93

Note: RSD is residual standard deviation and R is correlation coefficient deviation.

IV. SUMMARY

Water vapor plays an essential role in atmospheric dynamics, atmospheric thermodynamics and atmospheric chemistry. Because water vapor shows great spatial and temporal variability, its distribution is difficult to resolve by conventional means. Emerging networks of continuously operating GPS receivers offer the possibility of observing the horizontal distribution of IWV.

We investigated the strength of correlation between T_m and T_s by analyzing a set of **radiosonde** data obtained over one-year interval from stations in the eastern China, and **found a linear** relationship, for example, $T_m = 96.56 + 0.58T_s$ for September with a rms of **3.12 K scatter** about this regression. Thus it should be possible to predict the value of

IWV at a given place and time, given only surface temperature observations at the site.

Because of the strong linear correlation between T_m and T_s, and of the fact that most water vapor is located in the first 2 — 3 km of the atmosphere, they prompted us to consider operational prognostic mesoscale meteorological model, which predicts the three-dimensional distribution of meteorological variables with spatial resolution of 100 km and 16 vertical levels encompassing the entire eastern China. We obtain $T_m = 44.05 + 0.81T_s$ with a rsm of 2.96 K over one-year interval and in the grid domain.

The primary aim of this paper is to discuss the estimated method of T_m. The checking of relationship between T_m and T_s will be given in a future paper.

REFERENCES

Bevis, M. et al. (1992), GPS meteorology: Remote sensing of atmospheric water vapor using the global positioning system, *J. Geo. Res.*, **97**: 15 787—15 801.

Birnbaum, A. L. and Chatterjee, S. K. (1952), The dielectric constant of water vapor in the microwave region, *J. Appl. Phys.*, **23**: 220—223.

Boudouris, G. (1963), On the index of refraction of air, the absorption and dispersion of centimeter waves by gasses, *J. Res. Natl. Bur. Stand.*, **67**D: 631—684.

Davis, J. L., Herring, T. A., Shapiro, I. I., Rogers, A. E. E. and Elgered, G. (1985), Geodesy by radio interferometry: Effects of atmospheric modeling errors on estimates of baseline length, *Radio Science*, **20**: 1593—1607.

Elgered, G., Davis, J. L., Herring, T. A. and Shapiro, I. I. (1991), Geodesy by radio interferometry: Water vapor radiometry for estimation of the wet delay, *J. Geo. Res.*, **96**: 6541—6555.

Mao Jietai (1993), Meteorological apply of GPS, *Science and Technology of Meteorology*, **4**: 45—49 (in Chinese).

Owens, J. C. (1967), Optical refractive index air: dependence on pressure, temperature, and composition, *Appl. Opt.*, **6**: 51—58.

Thayer, D. (1974), An improved equation for the radio refractive index of air, *Radio Sci.*, **9**: 803—807.